

Relationship Explainable Multi-objective Reinforcement Learning with Semantic Explainability Generation *

Huixin Zhan¹ and Yongcan Cao¹

Abstract—Solving multi-objective optimization problems is important in various applications where users are interested in obtaining optimal policies subject to multiple, yet often conflicting objectives. A typical approach to obtain optimal policies is to first construct a loss function that is based on the scalarization of individual objectives, and then find the optimal policy that minimizes the loss. However, optimizing the scalarized (and weighted) loss does not necessarily provide guarantee of high performance on each possibly conflicting objective because it is challenging to assign the right weights without knowing the relationship among these objectives. Moreover, the effectiveness of these gradient descent algorithms is limited by the agent’s ability to explain their decisions and actions to human users. The purpose of this study is two-fold. First, we propose a vector value function based multi-objective reinforcement learning (V2f-MORL) approach that seeks to quantify the inter-objective relationship via reinforcement learning (RL) when the impact of one objective on others is unknown a priori. In particular, we construct one actor and multiple critics that can co-learn the policy and inter-objective relationship matrix (IORM), quantifying the impact of objectives on each other, in an iterative way. Second, we provide a semantic representation that can uncover the trade-off of decision policies made by users to reconcile conflicting objectives based on the proposed V2f-MORL approach for the explainability of the generated behaviors subject to given optimization objectives. We demonstrate the effectiveness of the proposed approach via a MuJoCo based robotics case study.

I. INTRODUCTION

In recent years, the application of RL in tasks with high-dimensional sensory inputs has shown the potential of creating artificial agents that can learn to accomplish a number of challenging tasks, including the Atari games [1], [2], [3], [4], [5], [6], [7], self-driving cars [8], and Go [9], [10], [11]. However, the approaches developed therein mainly focus on finding a single usable strategy, without considering the trade-off among potential alternatives that can increase one objective’s value at the cost of another.

In the multi-objective setting, the completion of a task requires the simultaneous satisfaction of multiple objectives such as balancing the power consumption and performance in Web servers [12]. Such problems can be modeled as multi-objective Markov decision processes (MOMDPs) and solved by some existing multi-objective reinforcement learning (MORL) algorithms [12], [13], [14]. However, solutions obtained via these approaches can hardly balance the possibly conflicting objectives to achieve satisfactory performance on all objectives.

Recently, several interesting MORL approaches have been developed. The author in [15] proposed the use of both linear weighted sum and nonlinear thresholded lexicographic ordering methods to develop a multi-objective deep RL framework that includes both single- and multi-policy strategies. The author in [16] proposed an architecture in which separated deep Q-networks (DQNs) are used to control the agent’s behavior with respect to particular objectives. Then, each DQN has an additional decision value output that acts as a dynamic weight used while summing up Q-values. The authors in [17] used softmax-epsilon selection based on a nonlinear action-selection operator. The agents incorporate an action-selection function that is defined as an ordering over these Q-values. In summary, most of the algorithms are based on the scalarization method to transform the multi-objective problem into a single objective one. The scalarization can be nonlinear or linear [15], [16], [17], [18]. Other advanced methods include, e.g., the convex hull [19], the varying parameters approaches [20], the constraint method [21], the sequential method [22], and the max-min method [23].

The authors in [24] proposed an upper bound for the multi-objective loss and proved that optimizing this upper bound via gradient-based multi-objective optimization yields a Pareto optimal solution. The Frank-Wolfe solver is used to find a minimum-norm point in the convex hull of the set of input points. This work provides a new perspective for balancing objectives when the values for all objectives are considered as the min-norm points in the convex hull. This work showed success in large scale multi-label learning tasks. However, it is unclear if the method can be extended to complex continuous space planning tasks.

When the values for all possibly conflicting objectives are considered as a vector and balancing them is required, it is critical to train a policy and explain why a particular behavior is generated is the topic under study. To address the critical issue, this paper focuses on proposing an explainable V2f-MORL approach. The proposed research has three main contributions. First, we propose an approximate optimistic linear support algorithm (AOLS), which allows the quantification of inter-objective relationship using the inter-objective relationship matrix (IORM). Second, instead of using scalarized Q-value and the action selection approach based on the priority objective value, the proposed method supports vectorized objective state values. In particular, we propose the creation of multi-objective value functions that can be used sequentially in the training of the critics to update the objective state values and the training of the actor to update the control policy. Third, our method is

¹The authors are with the Department of Electrical and Computer Engineering, University of Texas, San Antonio, TX, 78249. {huixin.zhan, yongcan.cao}@utsa.edu

applicable in high-dimensional continuous action spaces with an explainable planning via natural language representation. To our best knowledge, this is the first time that actor critics with quantifiable inter-objective relationship are developed to solve MORL with semantic representation. We also show via one MuJoCo example that the proposed method outperforms the existing single objective optimization methods.

II. PRELIMINARIES

A. Multi-Objective Value Function

For a control policy π , we here propose the construction of a set of *multi-objective value functions* \mathcal{Y}_i^π , $i = 1, \dots, I$ via our defined IORM W as $\mathcal{Y}^\pi = [\mathcal{Y}_1^\pi, \dots, \mathcal{Y}_I^\pi] \in \mathbb{R}^I = W\mathbf{V}^\pi$, where $W \in \mathcal{R}^{I \times I}$ is the IORM, I is the number of objectives, $\mathbf{V}^\pi = [V_1^\pi, \dots, V_I^\pi]^T$ with V_i^π representing the state value for the i th objective subject to the control policy π . The i th row of W , given by $[w_{i1}, \dots, w_{iI}]$, characterizes how other objective values, $\{V_j^\pi | j \neq i\}$, impact the i th objective value V_i^π under the policy π . We here provide a formal definition of the multi-objective value function under the policy π .

Definition 1. *Each multi-objective value function is a cumulative sum of objective state values with additive specific impact elements of the form given by*

$$\mathcal{Y}_i^\pi [i_k] = \sum_{j=1}^I w_{ij} [i_k] V_j^\pi [i_k], \quad i = 1, \dots, I, \quad (1)$$

where w_{ij} is the weight quantifying the impact of V_j^π on V_i^π , i_k is the time step number, and k is the number of sequence.

B. Inter-objective Relationship Matrix (IORM)

Based on Definition 1, we define the *inter-objective relationship matrix (IORM)* as

$$W = [w_{ij}] \in \mathbb{R}^{I \times I}. \quad (2)$$

Because the impact of one objective on another objective is unknown *a priori*, an IORM can be assigned an initial value but it needs to be updated based on the input observation, denoted as \mathcal{X} , and a collection of objective value spaces, denoted as $\{\mathcal{Y}^i\}_{i \in [I]}$, for each objective value y^i with m input/output examples denoted as $(x_1^i, y_1^i), \dots, (x_m^i, y_m^i)$. In particular, IORM will be updated via numerous batches. During each batch, $I \times k$ time steps will be divided into I sequences. In the i_k th time step, m examples are trained to fit y^i , which is then used to update the objective state values V_i . $\{V_j^\pi [i_k]\}_{j \in [I]}$ is then used to update the i th row of the relationship matrix W . More detailed description of such an update process will be provided in Section III.

As a consequence, the vector value function $\mathcal{Y}^\pi = [\mathcal{Y}_i^\pi] \in \mathbb{R}^{I \times I}$, where \mathcal{Y}_i^π is defined in (1), can be updated via

$$\begin{bmatrix} \mathcal{Y}_1^\pi [k] \\ \vdots \\ \mathcal{Y}_n^\pi [k] \end{bmatrix} = W[k] \begin{bmatrix} V_1^\pi [k] \\ \vdots \\ V_n^\pi [k] \end{bmatrix}, \quad (3)$$

where $W[k]$ is the updated IORM at the k th time step.

III. PROPOSED METHOD

A. Multi-objective Decision Making

In this paper, we consider the problem when multiple objectives O_i , $i = 1, \dots, I$, need to be optimized for a given mission, where I denotes the number of objectives. For example, in robotic locomotion, maximizing forward velocity but minimizing joint torque and impact with the ground, result in a very large number of options to consider. We use $\mathbf{V}^\pi \in \mathbb{R}^{d \times 1} = [V_1^\pi, \dots, V_I^\pi]^T$, where $d \geq 2$, to represent the vector value function for O_i , $i = 1, \dots, I$, subject to the control policy π . A typical approach to optimize objectives O_i , $i = 1, \dots, I$, is to construct a scalarized value function of the form $V_w^\pi \in \mathbb{R}^1 = w\mathbf{V}^\pi$, where $w = [w_1, \dots, w_I]$ satisfying $w\mathbf{1} = 1$, $\mathbf{1}$ is an all-one column vector, and weight w_i specifies how much each objective contributes to the scalarized objective. A more general form of the scalarized value function is given by $V_w^\pi = f(w, V_1^\pi, \dots, V_I^\pi)$ [14], where $f(\cdot, \cdot)$ is a nonlinear function. Hence, a multi-objective optimization problem can be converted to a single-objective optimization problem.

These value functions map a multi-dimensional policy value to a scalar according to the preferred policy on decision making and preference elicitation. Since all objectives are desirable, V_w^π is monotonically increasing in all objectives. Given this monotonicity property, the solution set is a Pareto front, i.e., convex coverage set (CCS), that contains for any allowed policy π' with value V' , any policy that has a greater or equal value in all objectives [14]. CCS can quantify the relationship between different policies subject to a number of objectives because one policy can yield good performance for one objective while poor performance for another objective. For instance, for objective i_1 , solution θ is better when the loss $\hat{\mathcal{L}}^{i_1}(\theta_{V_{i_1}}, \theta_{V_{j_1}}) = -V_w^\pi < \hat{\mathcal{L}}^{i_1}(\bar{\theta}_{V_{i_1}}, \bar{\theta}_{V_{j_1}})$, while for objective i_2 , solution $\bar{\theta}$ is better when $\hat{\mathcal{L}}^{i_2}(\theta_{V_{i_2}}, \theta_{V_{j_2}}) > \hat{\mathcal{L}}^{i_2}(\bar{\theta}_{V_{i_2}}, \bar{\theta}_{V_{j_2}})$. CCS defines the set of vector objective state values that the optimal value must reside in because every other vector objective state value not in the set will not be the best choice since there exists at least one vector in CCS that is not smaller than it.

A formal definition of the convex coverage set is given below.

Definition 2. *The convex coverage set, denoted as CCS, is the set of all actions and associated payoff values that are optimal for some w of the scalarization function $f(w, V^\pi)$:*

$$\exists V \in \text{CCS} : \forall V' \in \pi : w^T V' \leq w^T V, \forall w \in \mathbb{R}^d, \quad (4)$$

where $u_w(\cdot)$ is the value when taking action a based on the weight w .

B. Multi-objective Reinforcement Learning (MORL)

We first introduce a few definitions that are needed in solving multi-objective optimization problems using (deep) reinforcement learning. Let a trajectory $\tau^i = \{q(x_1), q(x_{t+1}|x_t, a_t), H\}$ consist of a distribution over initial observations $q(x_1)$ with a transition distribution $q(x_{t+1}|x_t, a_t)$ and an episode length H . We define the loss

$\mathcal{L}(x_1, a_1, \dots, x_H, a_H)$ as the negated expected accumulated reward for a series of state-action pairs with length H given by

$$\mathcal{L}^i(f_{\theta_\pi}) = -E_{x_t, a_t \sim f_{\theta_\pi, \tau^i}} \sum_{t=1}^H R_i(x_t, a_t), i = 1, \dots, I \quad (5)$$

where E is the expectation operation, f_{θ_π, τ^i} is the action distribution function determined by the policy π that is assumed to be constructed using a neural network with θ_π acting as the weights. Another set of hyperparameter is needed to quantify the map from V_i^π to \mathcal{Y}^i defined as

$$f(V_i^\pi; w_{ii}, w_{ij}) : V_i^\pi \rightarrow \mathcal{Y}^i, \quad (6)$$

where w_{ii} and w_{ij} are the weights in the i th row of the IORM W .

C. W Update

We now provide a detailed description of how W is updated within a batch. First, let's define the map from \mathcal{X} to $\{\mathcal{Y}^i\}_{i \in |I|}$ in a parametric form as $f^i(x; \theta_{V_i}, \theta_{V_j}) : \mathcal{X} \rightarrow \{\mathcal{Y}^i\}_{i \in |I|}$, where θ_{V_i} and θ_{V_j} are the aggregated weights of weights θ_π and hyperparameters w_{ij} . The main idea to update W is to first obtain the CCS, then evaluate the marginal weights on the CCS, and finally use the best marginal weight to update W .

Because it is difficult to obtain the CCS directly, we employ the approximate optimistic linear support (AOLS) approach [25] to get an approximated set. The AOLS is a method that can gradually improve the approximation of the CCS. Given a maximum improvement threshold $\varepsilon > 0$, the AOLS algorithm can compute an approximated ε -optimal set, denoted as \overline{CCS} , which may diverge from the optimal undominated set by at most ε . Consequently, its *marginal weight* can be obtained. Before a complete undominated set is obtained, a partial CCS can be obtained by evaluating the largest improvement for weights via the priority queue of the marginal weight in this step. An element in the vector value function over a partial CCS is defined by $V_S^*(w) = \max_{V \in S} w \cdot V(s, \phi_V)$, where S is the partial CCS, $V(s, \phi_V)$ is the approximated objective state value vector based on the current critic networks using the current weights ϕ_V , and s is the current state.

AOLS always selects the marginal weight w that maximizes an optimistic upper bound on the difference between $V_{\overline{CCS}}(w)$ and $V_S^*(w)$, i.e., $V_{\overline{CCS}}(w) - V_S^*(w)$, which can be updated iteratively to obtain a more accurate $\max_w V_{\overline{CCS}}(w)$. The pseudocode for AOLS is shown in the Algorithm 1.

D. Value-function and Policy update

To obtain policy network and value function approximation network, we propose to adopt an actor-critic network with *one actor network* and *I critic networks*, where the actor network is used to maximize the objective state value and each critic network is used to map from the state action pair to \mathcal{Y}_i^π . Assume that the actor network with weights θ_π

Data: MOMDP: m , improvement threshold: ε

Result: CCS, Δ_{max}

S : empty partial CCS, W : empty list of explored

marginal weight, Q : an empty priority queue of the initial marginal weight, Δ_{max} : improvement

forall extreme weights of infinite priority $w_{max} = e_1$ **do**
| $Q.add(w_{max}, \infty)$

end

while $\neg Q.isEmpty() \wedge \neg timeOut$ **do**

| $w_i^j \leftarrow Q.pop()$

| $WV_{old} = WV_{old} \cup \left\{ \left(w_i^j, w_i^j \cdot V(s, \phi_V) \right) \right\}$

if $V(s, \phi_V) \notin S$ **then**

| $S \leftarrow S \cup \{V(s, \phi_V)\}$

| $W \leftarrow \text{recompute marginal weight } V_S^*(w)$

| **for** $K \in 1, \dots, len(w)$ **do**

| | **if** $e_K \neq W$ **then**

| | | $\text{return}(e_K, \infty)$

| | **end**

| **end**

| $V_{US}[\cdot] \leftarrow \forall \text{ weights in } W [\cdot], \text{ compute: } \max$

| $w_i^j[K] \cdot v(s, \phi_V)$

| subject to:

| $\forall \left(w_i^j[K], u \right) \in WV : w_i^j[K] \cdot v(s, \phi_V) \leq u + \varepsilon$

| $K \leftarrow \arg \max_K V_{US}[K] - V_S^*(W[K])$

| **if** $V_{US}[K] - V_S^*(W[K]) > \varepsilon$ **then**

| | $Q.add(W[K], V_{US}[K] - V_S^*(W[K]))$

| | **end**

| **end**

| $W \leftarrow W \cup \{W[K]\}$

end

Algorithm 1: function AOLS($m, \varepsilon, V(s, \phi_k)$)

generates actions via $a = \pi(s; \theta_\pi)$. The weights θ_π can be updated using policy gradient given by [26]:

$$\Delta \theta_\pi \sim \sum_k \nabla_{\theta_\pi} \log \pi_\theta(s_k, a_k) \delta_{k,t},$$

where $\delta_{k,t}$ is the expected value of the i th objective, also known as the temporal difference (TD) residual of \widehat{V}_i^π with discount γ [27], given by

$$\delta_{k,t} = r_i(s_{k,t}, a_{k,t}) + \gamma \widehat{V}_i^{\pi(\theta_\pi)}(s_{k,t+1}; \phi_{V_i}) - \widehat{V}_i^{\pi(\theta_\pi^-)}(s_k; \phi_{V_i}^-) \quad (7)$$

where $r_i(s_{k,t}, a_{k,t})$ is the immediate reward at the t th time step on the k th experience, $\widehat{V}_i^{\pi(\theta_\pi^-)}(s_{k,t}; \phi_{V_i}^-)$ is the approximation of the value function V_i based on the old weights θ_π^- for the actor network and the old weights $\phi_{V_i}^-$ for the i th critic network, and $\widehat{V}_i^{\pi(\theta_\pi)}(s_{k+1}; \phi_{V_i})$ is the approximation of the value function V_i based on the updated weights θ_π for the actor network and the updated weights ϕ_{V_i} for the i th critic network.

For the I critic networks, its i th neural network with hyperparameter ϕ_{V_i} is used to approximate each element in the vector value function $V_i^\pi(s)$. Assume that the critic function

is given by $V_i(s; \phi_{V_i})$ with ϕ_{V_i} serving as the weights. The weights can be updated via $\Delta_k \phi_{V_i} \sim -\nabla_{\phi_{V_i}} \sum_k \delta_{k,t}^2$.

In the standard TD-residual method, the value of one action evaluated via (7) is an incremental form of value iteration. The key drawback of the standard TD-residual method includes the need for a large number of samples and large variance of policy gradient estimate. To address these issues, an existing approach, called generalized advantage estimator (GAE) [28], can be used to evaluate the action advantages and perform the policy updates using proximal policy optimization [29], [30], [31]. The GAE is defined by:

$$\begin{aligned} \hat{A}_t^{GAE(\gamma, \lambda)} &= \lim_{H \rightarrow \infty} (1 - \lambda) \sum_{j=1}^H \lambda^{j-1} \sum_{k=1}^j \gamma^{j-1} \delta_{k,t+j-1} \\ &= \sum_{l=0}^H (\gamma \lambda)^l \delta_{k,t+l}, \end{aligned}$$

where $\lambda \in [0, 1]$ and $\gamma \in [0, 1]$ adjusts the bias-variance tradeoff of GAE.

After new weights of the advantage actor-critic network models are obtained, V^π can be obtained via new samples using the updated policy. Afterwards, the procedure in Subsection III-C can be implemented to obtain the updated W . The entire process will iterate until $V_{\overline{C\overline{S}}}(w) - V_S^*(w) < \epsilon$, where ϵ is a small threshold selected by users.

E. Explainable Planning Representation

To address the quantifiable inter-objective relationship in our algorithm, we adopt an explainable planning representation that enables automatic explanation of the planning rationale.

1) *Vocabulary for Quality Attributes (QA)*: We map QA analytic models to domain-specific vocabulary to be used to generate verbal explanation. The vocabulary includes ‘‘QA type’’, ‘‘optimization objective’’, and ‘‘QA property’’ for the description of standard QAs.

2) *QA Language Templates*: To generate verbal explanation of the objectives and the QA properties of a solution policy π^* , we use predefined natural-language templates. Table I shows an example of verbal explanation of QA objectives and properties.

TABLE I

VERBAL EXPLANATION OF QA OBJECTIVES AND PROPERTIES

QA Type	Optimization Objective	QA Property
Standard measurement	‘‘maximize the alive bonus’’	‘‘the expected alive bonus is 150’’

3) *Obtaining Alternative Policies*: Algorithm 2 outlines an approach for sampling alternative policies around the current policy. The key idea of the approach is to start with the QA values of the current solution policy $\pi : V_1^\pi(s), \dots, V_I^\pi(s)$. For each QA i , we determine a new value V'_i that is more preferable than $V_i^\pi(s)$. Then, we construct a new planning problem with $I - 1$ optimization objectives (namely, excluding the objective associated with the QA i),

resulting in a new multi-objective value function subject to the constraint that the QA i must be at least as good as V'_i . Next, we select an optimal, constraint-satisfying solution value under π' for the new planning problem. The new policy (respectively, state value) provides an alternative of the current policy (respectively, state value associated with the current policy). This procedure will be executed iteratively until we obtain up to M_i number of alternative policies for each i . The pseudocode of the algorithm is given below.

Data: current policy π , state s , $V_1^\pi(s), \dots, V_I^\pi(s)$, all $n - 1$ attribute value functions $V_{\setminus 1}^\pi(s), \dots, V_{\setminus I}^\pi(s)$, increment sizes of values $\Delta V_1, \dots, \Delta V_I$, maximum values M_{V_1}, \dots, M_{V_I} , maximum number of alternatives M_1, \dots, M_I

Result: A set of alternatives Π'

$\Pi' \leftarrow \emptyset$

$D \leftarrow$ attributes to be explored, e.g., $\{1, \dots, n\}$;

while $D \neq \emptyset$ **do**

$i \leftarrow$ remove an attribute from D

$count_i \leftarrow 0$

$V_i \leftarrow V_i^\pi(s)$

$V_{\setminus i} \leftarrow n - 1$ attribute value function on all

$V_{\setminus i}^\pi(s), j \neq i$

while $V_i \leq (M_{V_i} - \Delta V_i) \wedge count_i \leq M_i$ **do**

$V_i \leftarrow V_i + \Delta V_i$

$\pi : \bar{V}_i^\pi(s) \leftarrow$ all $\pi : V_j^\pi(s)$, where $j \neq i$

$V' \leftarrow \arg \max_V \bar{V}_{\setminus i}^\pi(s)$, subject to $V_{\setminus i}^\pi(s) \geq V_i(s)$

if V' exists **then**

$\Pi \leftarrow \Pi' \cup \{V'\}$

$count_i \leftarrow count_i + 1$

for $j \neq i$ **do**

if $V_j'^\pi(s) \geq V_j^\pi(s) + \Delta V_j$ **then**

$D \leftarrow D - \{j\}$

end

end

end

end

end

Algorithm 2: Pseudocode for the calculation of alternative multi-objective values (function AV2f($\pi, \mathbf{V}^\pi(s), s, \Delta V, M_V, M_i$))

4) *Semantic Explanation of Value Tradeoffs*: Our value justification indicates the amount of gain-loss in the QAs if one were to choose each alternative value under the current policy. It then indicates preference towards the current policy by arguing that such gain is not worth the loss, reflecting the QA utility models underlying the multi-objective value function. We use a predefined natural language template for generating verbal justification: ‘‘I could [improve these QAs to these values], by [carrying out this alternative policy] instead. However, this would [worsen these other QAs to these values]. I decided not to do that because [the improvement in these QAs] is not worth [the deterioration in these other QAs]’’.

F. Overall Algorithm

The pseudocode for the proposed V2f-MORL approach described in Subsections III-C, III-D, and III-E is given in the Algorithm 3.

Data: initial policy parameters θ_0 , initial value function parameters $\phi_0^{V_i}$, initial vectorized weights based on each objective w_{ij} , *CCS*

Result: PPO_Model

for $i = 1$ to I **do**

for $k = 0, 1, 2, \dots, K$ **do**

Collect set of trajectories $D_k^i = \{\tau_n^i\}$ by running policy $\pi_k = \pi(\theta_k)$ in the environment

Compute rewards-to-go \hat{R}_t

Update $V(s, \phi_k)$

Compute $w_{i[\cdot]}$ by function

AOLS($m, \varepsilon, V(s, \phi_k)$)

$V_i^{\phi_k} = w_{i[\cdot]} \times V(s, \phi_k)$

Compute advantage estimates \hat{A}_t^i using GAE method based on the current value function

$V_i^{\phi_k}$

Update the policy by maximizing the PPO-Clip objective:

$$\theta_{k+1} = \arg \max_{\theta} \frac{1}{|D_k^i| T} \sum_{\tau_n^i \in D_k^i} \sum_{t=0}^T \min \left(\frac{\pi_{\theta}(a_t | s_t)}{\pi_{\theta_k}(a_t | s_t)} A^{i, \pi_{\theta_k}}(s_t, a_t), g(\varepsilon, A^{i, \pi_{\theta_k}}(s_t, a_t)) \right)$$

via stochastic gradient ascent (e.g., Adam)

Fit value function by regression on mean-squared error:

$$\phi_{k+1}^{V_i} = \arg \min_{\phi_k^{V_i}} \frac{1}{|D_k^i| T} \sum_{\tau_n^i \in D_k^i} \sum_{t=0}^T \left(V_i^{\phi_k}(s_t) - \hat{R}_t^i \right)^2$$

via stochastic gradient descent.

$\Pi \leftarrow$ function AV2f ($\pi, \mathbf{V}^{\pi}(s), s, \Delta V, M_V, M_i$)

end

end

Algorithm 3: Pseudocode for the calculation of vectorized multi-objective values (V2f-MORL)

IV. EXPERIMENTS

A. Setup

We here select the testing environment Ant-v2 on the MuJoCo physics engine [32], and select four objectives: Reward Control (Rctrl), Reward Contact (Rcont), Reward Survive (Rsurv), and Reward Forward (Rfor). We use the proximal policy optimization clipping algorithm with $\epsilon = 0.2$ as the optimizer. The discounting factor is selected as $\gamma = 0.99$. One episode, characterizing the number of time steps of the vectorized environment per update, is chosen as 2048. For stabilization purposes, we execute parallel episodes in one batch. The batch size is chosen as the product of the episode size and the number of environment copies simulated in

parallel. The number of environment copies is selected as 8. The parameters are optimized using the Adam algorithm [33] and a learning rate of 3×10^{-4} . All of the experiments were performed using TensorFlow, which allows for automatic differentiation through the gradient updates [34].

The parametric form $f^i(x; \theta_{V_i}, \theta_{V_j}) : \mathcal{X} \rightarrow \{\mathcal{Y}^i\}_{i \in [I]}$, where θ_{V_i} is the objective specific weight and θ_{V_j} is the inter-objective weight, is a CNN whose structure is shown in Fig. 1. The architecture specification is given in Table II. The FC8 and FC4 correspond to the 8-action policy $\pi(\cdot | s_t)$ and the value function $V(s_t)$. In the experiments, the screen is resized to an $84 \times 84 \times 3$ RGB image as the network input.

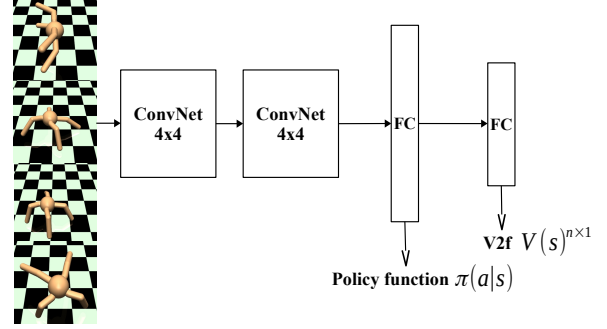


Fig. 1. The architecture of the shared parameter network

TABLE II
CNN ARCHITECTURE

Layer #	1	2	3	4
Parameters	$C4 \times 4 - 32S2$	$C4 \times 4 - 32S2$	FC8	FC4

B. Accuracy vs Episodes

We further investigated the effects of the number of training episodes (including series of time steps) on the maximal relative improvement of the CCS. Fig. 2 shows how the maximal relative improvement $\Delta_r(w) = \frac{V_{CCS}(w) - V_S^*(w)}{V_{CCS}(w)}$ of the CCS evolves with respect to the number of episodes. It can be seen from Fig. 2 that the error is highly affected by the number of training episodes. Although the proposed method is unable to provide sufficient accuracy to build the CCS initially, the deviation will gradually decrease to 0 when the number of episodes is 40.

C. Testing Results and Discussion

For the simplicity of presentation, we call our proposed method PPO_CCS method. To show the benefit of the proposed PPO_CCS method, we show the results when (1) multi-objective optimization is solved via one single-objective optimization, and (2) the marginal weight in our method is replaced by the corner points of the CCS. All these results are based on the MuJoCo simulator [32].

Our goal is to make a four-legged ant-v2 walk forward as fast as possible while saving cost simultaneously. More specifically, our goal is to maximize the reward forward and the reward survive while minimizing the reward control and

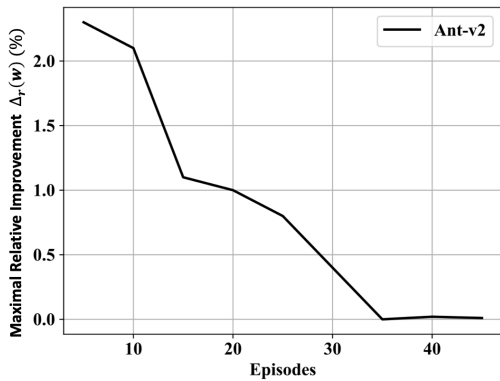


Fig. 2. Evolution of $\Delta_r(w)$ with respect to episodes in percentage

TABLE III
MULTI-OBJECTIVE VALUE FOR ANT-V2

	Single-objective		Multi-objective
	Rfor	Rsurv	PPO_CCS
Rsurv	76.341 ± 18.566	77.445 ± 14.542	92.546 ± 18.446
Rfor	0.541 ± 0.026	0.740 ± 0.057	0.818 ± 0.147
Rctrl	-4.011 ± 0.730	-4.019 ± 0.825	-5.025 ± 0.011
Rcont	-3.442 ± 0.250	-3.596 ± 0.011	$-4. \pm 0.023$

Average and standard deviation ($\mu \pm \sigma$) of multi-objective values.

the reward contact. We take the current reward function in the OpenAI Gym environments as a baseline, use the cumulative reward trained by the single objective PPO as a benchmark [35], [36], and compare it with our proposed method.

Table III shows the rewards using PPO_CCS and PPO with single objective. It can be observed that the proposed PPO_CCS yields higher reward. It can also be observed that PPO_CCS can generate higher rewards in most cases because PPO_CCS can optimize multiple objectives simultaneously, while the PPO with single objective does not seek to optimize multiple objectives.

D. Natural Language Representation Demonstration

We demonstrate three semantic representations that are generated under different policies using the proposed algorithm in Algorithm 2. The result is shown in Fig. 3. The first representation provides verbal explanation of the state values under the selected policy while the second and third representations provide verbal explanations why alternative policies were not selected. This is because the algorithm: (i) searched to reduce Rctrl on the CCS and found a different multi-objective value function that increases Rcont, decreases Rsurv, and decreases Rfor, and (ii) searched to reduce Rcont and found a different multi-objective value function that increases Rctrl, decreases Rsurv, and decreases Rfor.

V. CONCLUSIONS

In multi-objective optimization problems, the possibly conflicting objectives necessitates a trade-off when multiple objectives need to optimize simultaneously. A typical approach is to minimize a loss of weighted linear summation of all objective functions. However, this approach can hardly guarantee good performance on individual objectives because

“I aim to maximize the reward forward and the reward survive while minimizing the reward control and the reward contact. I plan to move forward. The Rctrl is -5.025, Rcont is -4, Rsurv is 92.546, and Rfor is 0.818.”

“I could decrease the Rctrl to -8.236, by move forward in another set of actions instead. However, this would decrease the Rcont by -1.953, decrease the Rsurv by 45.045, and decrease the Rfor by 0.417. I decided not to do that because the decrease in the Rctrl is not worth the increase of the Rcont, the decrease of the Rsurv, and the decrease of the Rfor.”

“I could also decrease the Rcont to -4.081, by move forward in another set of actions instead. However, this would decrease the Rctrl by -0.031, decrease the Rsurv by 7.882, and decrease the Rfor by 0.174. I decided not to do that because the decrease in the Rcont is not worth the increase of the Rctrl, the decrease of the Rsurv, and the decrease of the Rfor.”

Fig. 3. Natural language representation

it is very difficult to determine the right weights due to the lack of knowledge in inter-objective relationships. To address the challenge, we proposed a vector value function based multi-objective deep reinforcement learning to solve high-dimensional multi-objective decision making problems. The proposed method optimizes vectorized proxy objectives sequentially based on proximal policy optimization, actor-critical network, and the derivation of optimal weights via marginal weight.

By explicitly quantifying inter-objective relationship via relationship matrix, the relative importance of the objectives unknown *a priori* can be obtained via reinforcement learning. Each entry in the relationship matrix specifies and explains the relative impact of one objective on another objective in the optimization step. Moreover, in order to address the interpretability of the proposed V2f-MORL approach, we proposed a new approach to generate alternative multi-objective values/policies to automatically explain the rationale behind decided actions/policies.

REFERENCES

- [1] V. Mnih, K. Kavukcuoglu, D. Silver, A. A. Rusu, J. Veness, M. G. Bellemare, A. Graves, M. Riedmiller, A. K. Fidjeland, G. Ostrovski, et al., “Human-level control through deep reinforcement learning,” *Nature*, vol. 518, no. 7540, p. 529, 2015.
- [2] X. Guo, S. Singh, H. Lee, R. L. Lewis, and X. Wang, “Deep learning for real-time atari game play using offline monte-carlo tree search planning,” in *Advances in Neural Information Processing Systems*, 2014, pp. 3338–3346.
- [3] T. Schaul, J. Quan, I. Antonoglou, and D. Silver, “Prioritized experience replay,” *arXiv preprint arXiv:1511.05952*, 2015.
- [4] Z. Wang, T. Schaul, M. Hessel, H. Van Hasselt, M. Lanctot, and N. De Freitas, “Dueling network architectures for deep reinforcement learning,” in *Proceedings of the International Conference on International Conference on Machine Learning*, 2016, pp. 1995–2003.
- [5] H. Van Hasselt, A. Guez, and D. Silver, “Deep reinforcement learning with double q-learning,” in *AAAI*, vol. 2, 2016, p. 5.

- [6] J. Oh, X. Guo, H. Lee, R. L. Lewis, and S. Singh, "Action-conditional video prediction using deep networks in atari games," in *Advances in Neural Information Processing Systems*, 2015, pp. 2863–2871.
- [7] A. Nair, P. Srinivasan, S. Blackwell, C. Alcicek, R. Fearon, A. De Maria, V. Panneershelvam, M. Suleyman, C. Beattie, S. Petersen, *et al.*, "Massively parallel methods for deep reinforcement learning," *arXiv preprint arXiv:1507.04296*, 2015.
- [8] X. Pan, Y. You, Z. Wang, and C. Lu, "Virtual to real reinforcement learning for autonomous driving," *arXiv preprint arXiv:1704.03952*, 2017.
- [9] C. J. Maddison, A. Huang, I. Sutskever, and D. Silver, "Move evaluation in go using deep convolutional neural networks," *arXiv preprint arXiv:1412.6564*, 2014.
- [10] D. Silver, A. Huang, C. J. Maddison, A. Guez, L. Sifre, G. Van Den Driessche, J. Schrittwieser, I. Antonoglou, V. Panneershelvam, M. Lanctot, *et al.*, "Mastering the game of go with deep neural networks and tree search," *Nature*, vol. 529, no. 7587, p. 484, 2016.
- [11] D. Silver, T. Hubert, J. Schrittwieser, I. Antonoglou, M. Lai, A. Guez, M. Lanctot, L. Sifre, D. Kumaran, T. Graepel, *et al.*, "A general reinforcement learning algorithm that masters chess, shogi, and Go through self-play," *Science*, vol. 362, no. 6419, pp. 1140–1144, 2018.
- [12] G. Tesauro, R. Das, H. Chan, J. Kephart, D. Levine, F. Rawson, and C. Lefurgy, "Managing power consumption and performance of computing systems using reinforcement learning," in *Advances in Neural Information Processing Systems*, 2008, pp. 1497–1504.
- [13] P. Vamplew, R. Dazeley, A. Berry, R. Issabekov, and E. Dekker, "Empirical evaluation methods for multiobjective reinforcement learning algorithms," *Machine Learning*, vol. 84, no. 1-2, pp. 51–80, 2011.
- [14] D. M. Roijers, P. Vamplew, S. Whiteson, and R. Dazeley, "A survey of multi-objective sequential decision-making," *Journal of Artificial Intelligence Research*, vol. 48, pp. 67–113, 2013.
- [15] T. T. Nguyen, "A multi-objective deep reinforcement learning framework," *arXiv preprint arXiv:1803.02965*, 2018.
- [16] T. Tajmajer, "Modular multi-objective deep reinforcement learning with decision values," in *2018 Federated Conference on Computer Science and Information Systems (FedCSIS)*, 2018, pp. 85–93.
- [17] P. Vamplew, R. Dazeley, and C. Foale, "Softmax exploration strategies for multiobjective reinforcement learning," *Neurocomputing*, vol. 263, pp. 74–86, 2017.
- [18] K. Van Moffaert, M. M. Drugan, and A. Nowé, "Scalarized multi-objective reinforcement learning: Novel design techniques," in *AD-PRL*, 2013, pp. 191–199.
- [19] D. M. Roijers, S. Whiteson, and F. A. Oliehoek, "Computing convex coverage sets for faster multi-objective coordination," *Journal of Artificial Intelligence Research*, vol. 52, pp. 399–443, 2015.
- [20] C. Liu, X. Xu, and D. Hu, "Multiobjective reinforcement learning: A comprehensive overview," *IEEE Transactions on Systems, Man, and Cybernetics: Systems*, vol. 45, no. 3, pp. 385–398, 2015.
- [21] A. Konak, D. W. Coit, and A. E. Smith, "Multi-objective optimization using genetic algorithms: A tutorial," *Reliability Engineering & System Safety*, vol. 91, no. 9, pp. 992–1007, 2006.
- [22] H. Nakayama, Y. Yun, and M. Yoon, *Sequential approximate multiobjective optimization using computational intelligence*. Springer Science & Business Media, 2009.
- [23] J. G. Lin, "On min-norm and min-max methods of multi-objective optimization," *Mathematical programming*, vol. 103, no. 1, pp. 1–33, 2005.
- [24] O. Sener and V. Koltun, "Multi-task learning as multi-objective optimization," in *Advances in Neural Information Processing Systems*, 2018, pp. 527–538.
- [25] D. M. Roijers, J. Scharpf, M. T. Spaan, F. A. Oliehoek, M. De Weerd, S. Whiteson, *et al.*, "Bounded approximations for linear multi-objective planning under uncertainty," in *International Conference on Automated Planning and Scheduling*, 2014.
- [26] K. G. Vamvoudakis and F. L. Lewis, "Online actor-critic algorithm to solve the continuous-time infinite horizon optimal control problem," *Automatica*, vol. 46, no. 5, pp. 878–888, 2010.
- [27] R. S. Sutton and A. G. Barto, *Reinforcement learning: An introduction*. MIT press, 2018.
- [28] J. Schulman, P. Moritz, S. Levine, M. Jordan, and P. Abbeel, "High-dimensional continuous control using generalized advantage estimation," *arXiv preprint arXiv:1506.02438*, 2015.
- [29] J. Schulman, F. Wolski, P. Dhariwal, A. Radford, and O. Klimov, "Proximal policy optimization algorithms," *arXiv preprint arXiv:1707.06347*, 2017.
- [30] J. Schulman, S. Levine, P. Abbeel, M. Jordan, and P. Moritz, "Trust region policy optimization," in *International Conference on Machine Learning*, 2015, pp. 1889–1897.
- [31] R. T. Rockafellar and R. J.-B. Wets, "Scenarios and policy aggregation in optimization under uncertainty," *Mathematics of Operations Research*, vol. 16, no. 1, pp. 119–147, 1991.
- [32] E. Todorov, T. Erez, and Y. Tassa, "Mujoco: A physics engine for model-based control," in *International Conference on Intelligent Robots and Systems*, 2012, pp. 5026–5033.
- [33] D. P. Kingma and J. Ba, "Adam: A method for stochastic optimization," *arXiv preprint arXiv:1412.6980*, 2014.
- [34] M. Abadi, P. Barham, J. Chen, Z. Chen, A. Davis, J. Dean, M. Devin, S. Ghemawat, G. Irving, M. Isard, *et al.*, "Tensorflow: a system for large-scale machine learning," in *USENIX Symposium on Operating Systems Design and Implementation*, vol. 16, 2016, pp. 265–283.
- [35] G. Brockman, V. Cheung, L. Pettersson, J. Schneider, J. Schulman, J. Tang, and W. Zaremba, "Openai gym," *arXiv preprint arXiv:1606.01540*, 2016.
- [36] P. Dhariwal, C. Hesse, O. Klimov, A. Nichol, M. Plappert, A. Radford, J. Schulman, S. Sidor, and Y. Wu, "Openai baselines," *GitHub, GitHub repository*, 2017.